Supporting information

An allosteric key strand controlled adaptable CRISPR/Cas12a biosensing platform for point-of-care testing of multiple types of targets

Juan Li[a], Tong Shao[a], Xin-Jiao Cao[a], Ya-Xin Wang[a]*, De-Ming Kong[b].

[a]*School of Pharmacy, Binzhou Medical University, Yantai, Shandong, 264003, PR China*

[b]*College of Chemistry, Nankai University, Tianjin, 300071, PR China.*

**Corresponding author: yaxinwang@bzmc.edu.cn*

1. Experimental section

1.1 Materials and reagents.

All LS sequences and crRNA sequences used in this experiment were synthesized and purified by Gen Script Biotechnology Co., Ltd. (Nanjing, China). Other DNA oligonucleotide sequences were synthesized and purified by Sangon Biotechnology Co., Ltd. (Shanghai, China) (Table S1). EnGen® Lba Cas12a (Cpf1) nuclease (M0653T), 10× NEBuffer 2.1 buffer (500 mM NaCl, 100 mM Tris-HCl, 100 mM $MgCl_2$, 100 μg/mL BSA, pH 7.9) (B6002). $Na_2HPO_412H_2O$ (10020328) and KH_2PO_4 (10017618) were purchased from Sinopharm Group Chemical Reagent Co., LTD. (Shanghai, China). KCl (7447-40-7) was purchased from the Sinopharm Chemical Reagents Network. $MgCl_2$ (7786-30-3) was secured from Shanghai Maclin Biochemical Technology Co., LTD. (China, Shanghai). NaCl (7647-14-5) was purchased from Tianjin Beilian Fine Chemical Development Co., LTD. (Tianjin, China). Endonuclease IV (M0304), NEBuffer™3 (100 mM NaCl, 50 mM Tris-HCl, 10 mM $MgCl_2$, 1 mM DTT, pH 7.9), Uracil glycosylase Inhibitor (UGI) (M0281), Human Alkyl Adenine DNA Glycosylase (HAAG) (M0313) were purchased from New England Biolabs (Beijing, China). Kanamycin sulfate (KAN) (B25656) was purchased from Shanghai Yuanye Biotechnology Parts Co., Ltd. (Shanghai, China). Chlortetracycline (Chl) (100940-65-6), oxytetracycline (Oxy) (6153-64-6), levofloxacin (Lev) (100986-85-4), doxycycline hydrochloride (Dox) (10592-13-9), and enrofloxacin (Enr) (93106-60-6) were purchased from Aladdin Biochemical Technology Co., Ltd. (Shanghai, China). 30% Rubber liquid, Uracil DNA glycosidase (UDG) (U8181), and Recombinant human OGG1 (OGG1) (P02796) were purchased from Beijing Solarbio Technology Co., LTD. (Beijing, China). Tetramethylethylenediamine (TEMED), Ammonium persulphate (APS), BeyoAP Alkaline Phosphatase (ALP) (D7027), T4 Polynucleotide Kinase (T4 PNK) (D7096), Protein Standard (BSA) (P0007), and Western and IP cell lysates were purchased from

Beyotime Biological Co., LTD. (Shanghai, China). 20bp DNA Ladder (Japan Takara), 6× DNA loading buffer (Kangwei Jiangsu), Super GelRed Nucleic acid dye (US Everbright). Cas12/13 special nucleic acid test strip was purchased from Guangzhou Bio-lifesci Biotechnology Co., Ltd. (Guangzhou, China). 10% FBS, 1% double-antibody (Penicillin-Streptomycin), DEME medium, cells were used in PBS and diethyl coke carbonate (DEPC) prepared and diluted from Sangon Biotechnology Co., Ltd. (Shanghai, China). Serum from healthy clinical human samples was provided by Yantai Affiliated Hospital of Binzhou Medical College (Yantai, Shandong). **293T cells, A549 cells, MB-231 cells, and MCF-7 cells were from Cell Bank/Stem Cell Bank, Chinese Academy of Sciences (Shanghai, China).** All other reagents were of analytical grade without requiring further purification.

Table S1 All DNA and RNA sequences

Name	**Sequence (5'-3')**
LS-5	CTATCTATGTGAGGTAGGTGGTATAGTCAAAACTATACCACCTACCTCACATA
LS-7	CCCTATCTATGTGAGGTAGGTGGTATAGTCAAAACTATACCACCTACCTCACATA
LS-10	TTACCCTATCTATGTGAGGTAGGTGGTATAGTCAAAACTATACCACCTACCTCACATA
LS-12	TCTTACCCTATCTATGTGAGGTAGGTGGTATAGTCAAAACTATACCACCTACCTCACATA
LS-16	CTTCTCTTACCCTATCTATGTGAGGTAGGTGGTATAGTCAAAACTATACCACCTACCTCACATA
LS-18	CTCTTCTCTTACCCTATCTATGTGAGGTAGGTGGTATAGTCAAAACTATACCACCTACCTCACATA
LS-20	CTCTCTTCTCTTACCCTATCTATGTGAGGTAGGTGGTATAGTCAAAACTATACCACCTACCTCACATA
LS-R	CTCTTCTCTTACCCTATCTATGTGAGGTAGGTGGTATAGTCAAAACTATACCAC**A**TACCTCACATA
LS-L	CTCTTCTCTTACCCTATCTATGTGAGGTAGGTGGTATAGTCAAAACTATACCACCTACCTCA**C**ATA
KS-5	TTTGACTATACCACCTACCTCACA TAGATAG
KS-7	TTTGACTATACCACCTACCTCACA TAGATAGGG
KS-10	TTTGACTATACCACCTACCTCACA TAGATAGGGTAA
KS-12	TTTGACTATACCACCTACCTCACA TAGATAGGGTAAGA

KS-16	TTTGACTATACCACCTACCTCACA TAGATAGGGTAAGAGAAG
KS-18	TTTGACTATACCACCTACCTCACA TAGATAGGGTAAGAGAAGAG
KS-20	TTTGACTATACCACCTACCTCACA TAGATAGGGTAAGAGAAGAGAG
KS	TTTGACTATACCACCTACCTCACA TAGATAGGGTAAGAGAAGAG
2-KS	GT TTTGACTATACCACCTACCTCACA TAGATAGGGTAAGAGAAGAG
4-KS	TAGT TTTGACTATACCACCTACCTCACA TAGATAGGGTAAGAGAAGAG
HPV-16	AATATGTCATTATGTGCTGCCATATCTACTTCAGAAACT
KS-H1	TTTGACTATACCACCTACCTCACATATTTTTTTTTTGCAGCACATAATGA CATATT
KS-H2	AGTTTCTGAAGTAGATATGTTTTTTTTTT GATAGGGTAAGAGAAGAG
Mis1	AATATGTCATTATGTGCTGCCATAGCTACTTCAGAAACT
Mis2	AATATGTCATTATGTGCAGCCATAGCTACTTCAGAAACT
Mis3	AATATGTCATTATGTGCAGCCATAGCTACTCCAGAAACT
HPV-51	TCTGCTGTACAACGCGAAGG
HPV-18	GTATATTGCAAGACAGTATTGGAACTTACAGAGG
HPV-58	ACAGCTAGGGCACACAATGG
KS-K1	TTTGACTATACCACCTACCTCACATA GCGCGCGC GGGACTTGGTTTA
KS-K2	GGTAATGAGTCCC CACGCGTG GATAGGGTAAGAGAAGAG
KS-U	TTUCTCUTTACCUCTATTTTTGACTATACCACCTACCTCACATAGATAGG GTAAGAGAAGAG
miR-21	TAGCTTATCAGACTGATGTTGA
KS-R1	TTTGACTATACCACCTACCTCACATATTTTTTTTTTCTGATAAGCTA
KS-R2	TCAACATCAGTTTTTTTTTTT GATAGGGTAAGAGAAGAG
KS-A1	TTTGACTATACCACCTACCTCACATAGCGCGCGCGACCTGGGGGAGTA
KS-A2	TTGCGGAGGAAGGCACGCGTGGATAGGGTAAGAGAAGAG
KS-M	TTSCTCSTTACCSCTATTTTTGACTATACCACCTACCTCACATAGATAGGG TAAGAGAAGAG
FB-S1	FAM-TTATT-BHQ-1
FAM-S2	TCTTCATCTTCATCTCTCAGTGTAGAGAGATGAAGATGAAGACTGGTT-6'FAM
crRNA	UAAUUUCUACUAAGUGUAGAUACUAUACCACCUACCUCACAUA
LFA-S3	FAM-TTATT-Biotin

In the above table, the red fonts are the Toehold sequence and the complementary sequence; The yellow highlighted base is divided into PAM and complementary sequences. The bases in blue are the KS chain 5'redundant complementary sequence. The underlined part of the solid line indicates the complementary domain of HPV-16 in KS-H1 and KS-H2 (miR-21 in KS-R1 and KS-R2). The underlined part of the dotted line indicates the aptamer sequence bound to kanamycin in KS-K1 and KS-K2 (ATP in KS-A1 and KS-A2). The bases in green are the uracil base sites in KS-U and thio sites in KS-M.

1.2 Apparatus.

TU-1901 dual-beam UV spectrophotometer was purchased from General Instruments Co., Ltd. (Beijing, China). PC-96 gradient PCR instrument was acquired from Yuning Instrument Co., Ltd. (Hangzhou, China). F97 Fluorescence spectrophotometer was applied from Light Technology Co., Ltd. (Shanghai, China). PowerPac Basic Electrophoresis instrument was purchased from BIO-RAD Company (USA). Automatic CDD gel imaging system was purchased from Tianeng Technology Co., Ltd. (Shanghai, China). EL 204 electronic balance, FE28 pH purchased from Mettler-Toldo Instruments Co., Ltd. (Shanghai, China). The Mini-10K high-speed centrifuge was recorded from Shuke Instrument Co., Ltd. (Sichuan, China). G560E vortex mixer was cultured from Scientific Industries Limited (USA).

1.3 Non-denaturing polyacrylamide gel electrophoresis

The trans-cis cleavage activity of the three targets was validated by non-denaturing polyacrylamide gel electrophoresis using the constructed 'lock-in hairpin + V-KS' mode biosensor. 1 μM KS-H1, 1 μM KS-H2, 1 μM HPV-16 and 2 μM LS were added for HPV-16 detection. 1 μM KS-K1,1 μM KS-K2,1 μM KAN and 1.5 μM LS were added for KAN detection. 1 μM KS-U, 1 U/mL UDG, 4 U/mL End IV and 1 μM LS were added for UDG detection. Finally, add 200 nM RNP and 50 μM FAM single-label fluorescence (FAM-S2). After the reaction was completed, 2 μL 6× loading buffer was added to the system. The mixture was evenly mixed and added into the 15% gel electrophoresis hole. The electrophoresis was run in 1× TAE buffer (40 mM Tris-acetic acid solution, 2 mM EDTA, pH 8.0), maintaining 1 hour at 120 V voltage. Then, the gel was placed in the gel imager for imaging observation.

1.4 Fluorescence experiments

Before detecting the classification target, we conducted feasibility verification on the whole system. LS (30 nM), RNP (20 nM), NEBuffer 2.1, FB-S1 (500 nM), and different concentrations of KS were added to a total volume of 30 μL. The mixed system was incubated in the amplification apparatus at 37℃ for 1 hour and then supplemented with DEPC water to a final volume of 100 μL. After vortex mixing, the samples were detected by fluorescence. F represents the fluorescence intensity of the sensor with target, while F_0 represents the fluorescence intensity of the sensor without target.

1.5 Recovery experiment

For the nucleic acid target HPV-16 detection, different concentrations of HPV-16 (10 nM, 25 nM,

40 nM) were added to the serum from diluted healthy human samples, and 3.6 μL KS-H1, 3.6 μL KS-H2, and 1.5 μL NEBuffer 2.1 buffers were added to a final volume of 15 μL. The rest of the reaction steps are the same as in 1.4 above.

For the small-molecule target kanamycin, different concentrations (10 nM, 50nM, 100 nM, 20 μM, 30 μM, 45 μM) of KAN were added to Yili pure milk (Yantai Laishan Zhenhua Supermarket) and school lake water (Yantai Laishan) after a 50-fold dilution. Then 3 μL KS-K1, 3 μL KS-K2, and 1.5 μL PBS buffer were added to the samples for a total volume of 15 μL. The rest of the reaction steps are the same as in 1.4 above.

According to the formula:

Sample spike recovery%= (measured-blank) / spike * 100%,

RSD% = S /$\bar{X}$ (S is the standard deviation, $\bar{X}$ is the measured mean)

1.6 Analysis of UDG activity in cell lysate

Human embryonic kidney cells (293T), human non-small cell lung cancer cells (A549), human breast cancer cells (MB-231), and human breast cancer cells (MCF-7) were cultured in DMEM medium supplemented with 10% FBS and 1% double antibody at 37℃ in a humid atmosphere containing 5% CO_2.

When the cell density in the petri dish reached 80%, the cells were centrifuged and the supernatant was discarded. After the cells were washed twice with PBS, 100 μL Western and IP cell lysate (contains 20 mM Tris-HCl, 1 mM PMSF, 150 mM NaCl, 1% Triton X-100, sodium pyrophosphate, β-glycerophosphate, EDTA, Na_3VO_4, and leupeptin, pH 7.5) was incubated with the washed cells. Then the mixture was placed on ice, and the vortex was oscillated for 15 seconds after removing every 5 minutes. This step was repeated six times. After completion, the cell extract was centrifuged at 12000 rpm at 4℃, and the obtained cell extract was directly used for UDG analysis or stored in sub-packaging at -80℃.

2. Allosteric key strand activated CRISPR/Cas12a biosensor

2.1 Verify the feasibility of the CRISPR trans-cleavage system

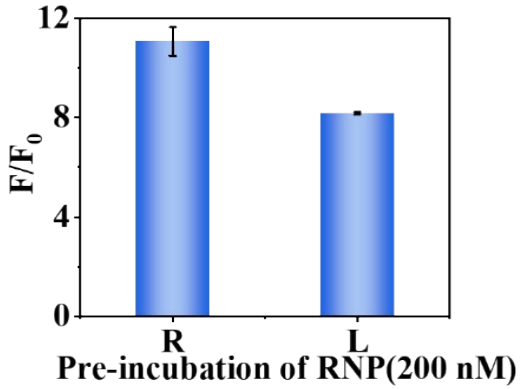

Fig.S1 The F/F_0 results of RNP incubation in advance (0.5 hours at 37℃). Error bars represent the standard deviation of three repetitive experiments.

As shown in Fig. S1, pre-incubating LbCas12a with crRNA resulted in a higher F/F_0 ratio of the sensor. This improvement can be attributed to the fact that the cleavage activity of CRISPR/Cas12a requires the formation of a complex between LbCas12a and crRNA. Pre-incubation facilitates this binding prior to the reaction, thereby reducing the time required for complex formation during the cleavage process and enhancing the overall efficiency.

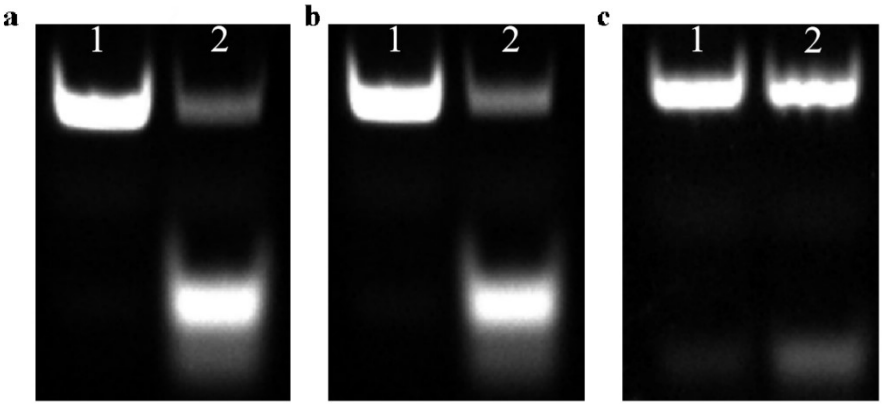

Fig.S2. PAGE validation of three types of targets. **(a)** Line 1: KS-H1+KS-H2+LS+RNP+FAM-S2, Line 2: HPV-16+KS-H1+KS-H2+LS+RNP+FAM-S2. **(b)** Line 1: KS-K1+KS-K2+LS+RNP+FAM-S2, Line 2: KAN+KS-H1+KS-H2+LS+RNP+FAM-S2. **(c)** Line 1: KS-U+EndIV+LS+RNP+FAM-S2, Line 2: UDG+KS-U+End IV+LS+RNP+FAM-S2.

After the KS sequence was exposed to different types of targets allosterism, trans-cleavage activity of CRISPR/Cas12a was confirmed by PAGE analysis. As shown in Fig. S2a, in the presence of the small molecule HPV-16, a new cleaved FAM-S2 band appears below lane 2. Similarly, as shown in Fig. S2b, the addition of KAN also results in a cleavage product migrating below lane 2. Furthermore, as depicted in Fig. S2c, when UDG is present, a cleaved FAM-S2 fragment is also observed below lane 2.

2.2 Optimization of reaction conditions for HPV-16 detection

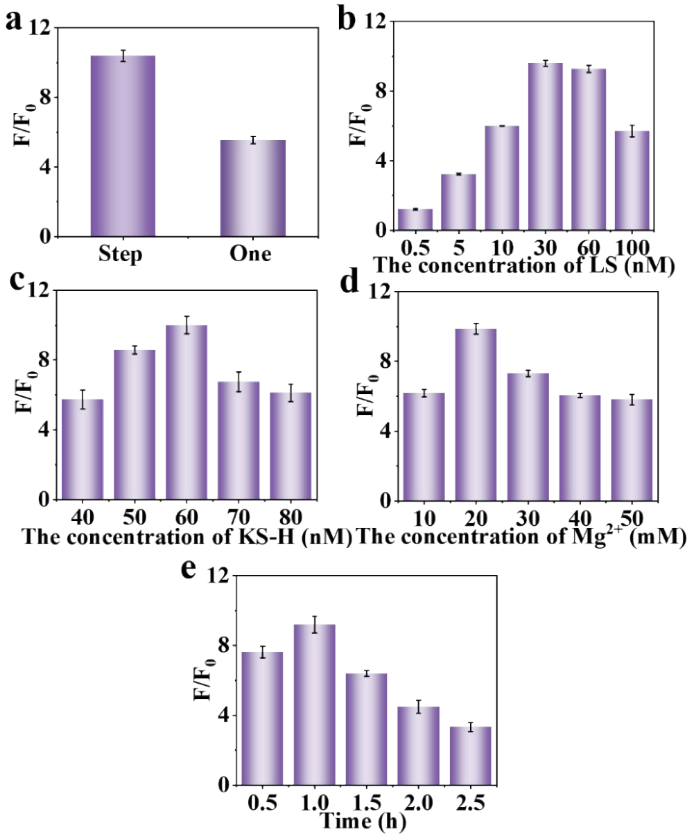

Fig.S3. Optimization of HPV-16 sensing system. **(a)** The F/F_0 value of target binding and trans-cleavage compared with one one-pot method. **(b)** F/F_0 values of different LS probe concentrations. **(c)** F/F_0 values of different KS-H cleavage probes at different concentrations. **(d)** F/F_0 value at different Mg^{2+} concentrations. **(e)** F/F_0 values of HPV-16 at different reaction times. (The target concentration of HPV-16 was 50 nM). Error bars represent the standard deviation of three repetitive experiments.

As shown in Fig. S3a, the stepwise method has a higher F/F_0 result than the one-pot method. Therefore, the target binding and trans-cleavage are performed step by step. As shown in Fig. S3b, in the HPV-16 sensing system, the F/F_0 signal is strongest when the probe LS concentration is 30 nM. As shown in Fig. S3c, the F/F_0 signal was strongest when the concentration of split probe KS-H1/H2 was 60 nM. As shown in Fig. S3d, the F/F_0 signal is strongest when the concentration of magnesium ions in the buffer solution is 20 mM. As shown in Fig. S3e, the optimal reaction time is 1 hour.

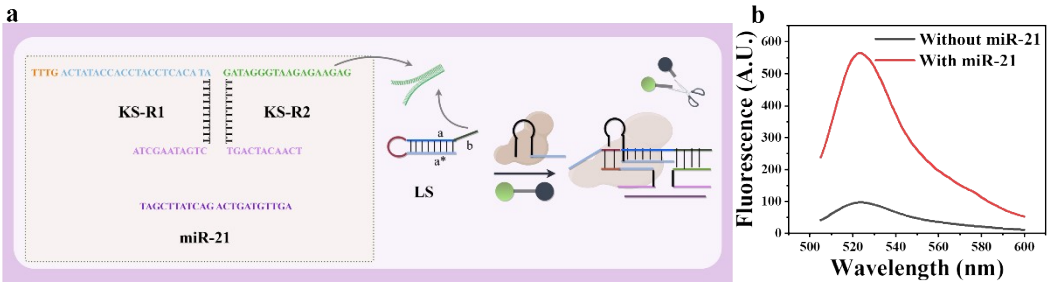

Fig.S4. **(a)** Schematic representation and working principle of miR-21 detection. **(b)** Fluorescence intensity of CRISPR/Cas12a biosensor with/without miR-21 (100 nM).

To validate the applicability of the proposed CRISPR/Cas12a biosensor and experimental conditions in detecting other nucleic acid targets, we chose another tumor marker, microRNA-21 (miR-21), as a test sample. Since the recognition of HPV by the CRISPR/Cas12a sensor is based on the complementary base-pairing of nucleic acids, we merely substituted the sequences in KS-H1 and KS-H2 that are complementary to HPV-16 with the corresponding sequences complementary to miR-21, designated as KS-R1 and KS-R2, while keeping the other regions intact (Fig.S4a). Consequently, both the cleavage site (the interval where the KS sequence splits into two parts) and the spacer arm sequence are the same as those of HPV-16. The complementary base sequences were attached to the 3' end of KS-R1 and the 5' end of KS-R2 according to the sequence of miR-21. In Fig S4b, we selected 100 nM of miR-21 for verification. The experimental conditions were precisely the same as those employed for the detection of HPV-16. The experimental results indicated that the fluorescence signal value was higher in the presence of the target miR-21. Thus, the experiment with miR-21 verified that the CRISPR/Cas12a biosensor were applicable to other nucleic acid targets.

2.3 Table S2. Recovery of HPV-16 detection in serum from human samples

Additon (nmol/L)	Detection (nmol/L)			Recovery (%)	RSD (%)
	1	2	3		
10	9.06	9.31	8.65	90.07	3.70
25	26.20	25.73	28.37	107.07	5.26
40	38.00	37.57	40.25	96.52	3.73

Each group of samples were run in parallel three times (error bars n=3)

2.4 Optimization of reaction conditions for KAN detection

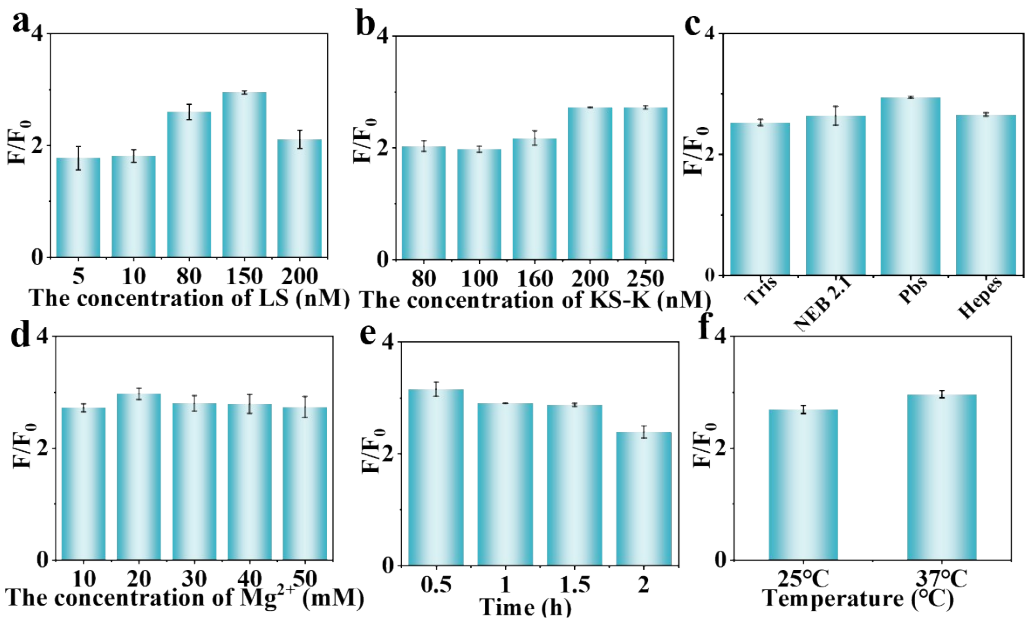

Fig.S5. Optimization of KAN sensing system. **(a)** F/F_0 values of different LS probe concentrations. **(b)** F/F_0 values of different KS-K cleavage probes at different concentrations. **(c)** The F/F_0 results of KAN binding to different types of buffer solutions. **(d)** F/F_0 value at different Mg^{2+} concentrations. **(e)** F/F_0 values of KAN at different reaction times. **(f)** The F/F_0 value of KAN binding was affected by different reaction temperatures. (The target concentration of KAN was 100 nM). Error bars represent the standard deviation of three repetitive experiments.

As shown in Fig. S5, in the KAN sensing system, the F/F_0 signal is strongest when the probe LS concentration is 150 nM. The F/F_0 signal was strongest when the concentration of split probe KS-K1/K2 was 200 nM. The F/F_0 of PBS buffer was slightly higher, and all subsequent experiments were conducted with PBS buffer. The F/F_0 signal is strongest when the concentration of magnesium ions in the buffer solution is 20 mM. The optimal reaction time is 0.5 hours, and the optimal reaction temperature is 37℃.

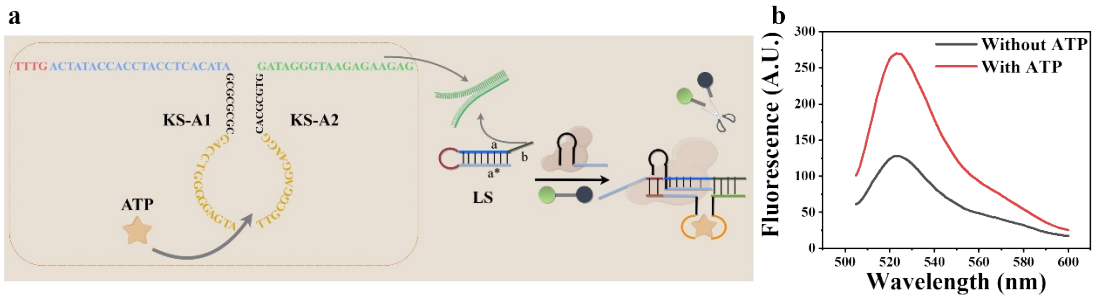

Fig.S6. **(a)** Schematic representation and working principle of ATP detection. **(b)** Fluorescence intensity of CRISPR/Cas12a biosensor with/without ATP (200 μM).

To validate the applicability of the proposed CRISPR/Cas12a biosensor and experimental conditions in the detection of other small molecules, we chose another important biomarker with specific aptamer, ATP, as a test sample. Based on the split ATP aptamers in previous work,[1] the KS chain was transformed into KS-A1 and KS-A2 by replacing the KAN aptamer sequence of KAN-CRISPR/Cas12a biosensor (KS-K1 and KS-K2) with ATP aptamer (Fig.S6a). Similarly, the ATP aptamer sequences were ligated to the 3'end of KS-A1 and the 5' end of KS-A2 respectively, forming a complete ATP aptamer sequence in the presence of a target. The PAM sequences of KS-A1 and KS-A2 are identical, with their a* and b* sequences being completely the same. We selected 200 μM ATP to validate the feasibility of CRISPR/Cas12a biosensor in ATP detection. Except for the buffer solution of the ATP-binding aptamer in the first step being different, all other experimental conditions are the same as KAN detection. The MES buffer (1 M NaCl, 20 mM Mg^{2+},10 mM MES, pH 7.2) solution was selected as the buffer, which is a mature method reported in the literature[2] and previously validated by our research group. The experimental results indicated that the fluorescence signal value was higher in the presence of the target ATP. Thus, the experiment with ATP verified that the CRISPR/Cas12a biosensor were applicable to other small molecules.

2.5 Table S3. Detection of recovery of KAN in pure milk and lake water

Add (nmol/L)		Detection (nmol/L)			Recovery （%）	RSD （%）
		1	2	3		
pure milk	10	13.46	14.33	15.12	106.13	3.53
	50	51.10	61.81	69.76	106.89	5.09
	100	119.21	105.28	105.27	107.93	3.46
lake water	10	4.57	11.34	9.13	98.75	2.63
	50	44.25	37.72	53.78	97.78	4.81
	100	82.36	109.13	111.49	103.79	7.23

Add (μmol/L)		Detection (μmol/L)			Recovery （%）	RSD （%）
		1	2	3		
pure milk	20	19.36	22.75	19.42	102.56	9.46
	30	33.19	30.01	33.35	107.28	5.85
	45	51.53	49.90	49.30	111.56	2.30
lake water	20	21.44	19.80	22.26	105.83	5.92
	30	28.49	26.52	26.85	90.96	3.87
	45	48.04	49.35	49.30	108.66	1.52

Each group of samples were run in parallel three times (error bars n=3)

2.6 Optimization of UDG detection reaction conditions

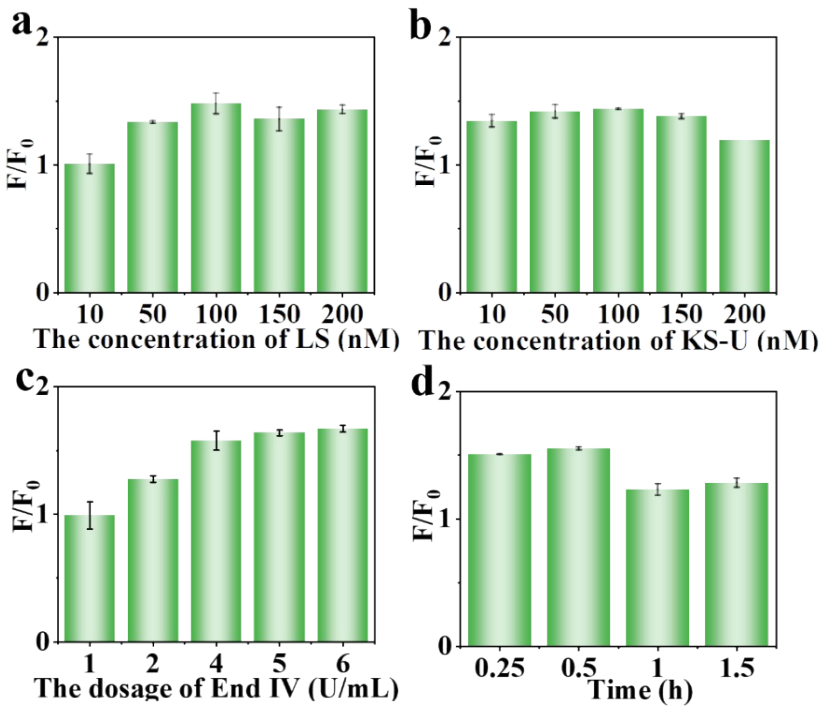

Fig.S7. Optimization of UDG sensing system. **(a)** F/F_0 values of different LS probe concentrations. **(b)** F/F_0 values of different KS-U cleavage probes at different concentrations. **(c)** F/F_0 values of nucleases with different concentrations. **(d)** F/F_0 values of UDG at different reaction times. (The target concentration of UDG was 1 U/mL). Error bars represent the standard deviation of three repetitive experiments.

As shown in Fig. S7a, the F/F_0 signal is strongest in the UDG sensing system when the probe LS concentration reaches 100 nM. Similarly, as presented in Fig. S7b, the maximum F/F_0 signal is observed when the KS-U concentration is 100 nM. According to Fig. S7c, the highest F/F_0 signal is achieved with an End IV concentration of 4 U/mL. Finally, as illustrated in Fig. S7d, the optimal reaction time is determined to be 0.5 hours.

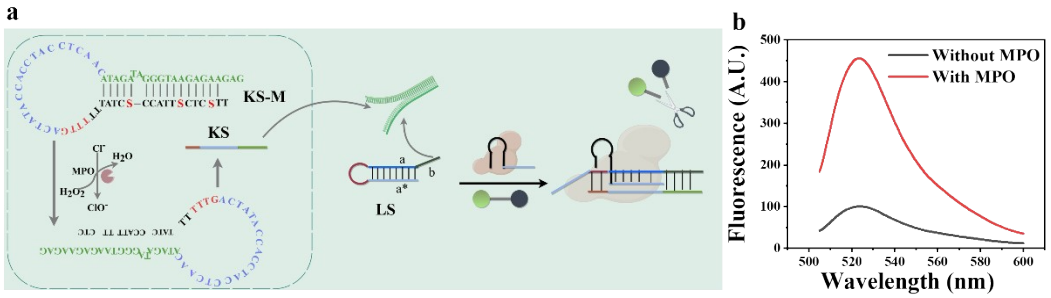

Fig.S8. **(a)** Schematic representation and working principle of MPO detection. **(b)** Fluorescence intensity of CRISPR/Cas12a biosensor with/without MPO (200 ng/mL).

To validate the applicability of the proposed CRISPR/Cas12a biosensor and experimental conditions in the detection of other enzymes with specific cleavage sites, we chose another important bio markers of cardiovascular diseases, myeloperoxidase (MPO), as a test sample. The sequence design of MPO maintains the stable hairpin structure identical to KS-U, in which the three U bases are replaced with thiol sites, named as KS-M (Fig.S8a). MPO catalyzes the cleavage of thiol sites by generating ClO^- from H_2O_2 and Cl^-.[3] Subsequently, the stem of the KS-M hairpin structure is destroyed, causing the hairpin to unfold and release KS. In the KS-M sequence, the PAM and a* sequences are also fixed at the hairpin loop, while the b* sequence serves as the stem to stabilize the hairpin structure. In Fig S8b, we selected 200 ng/mL MPO to validate the feasibility of CRISPR/Cas12a biosensor in MPO detection. All other experimental conditions are the same as UDG detection, except for the buffer solution of the enzyme cleavage in the first step. 200 μM H_2O_2 and 1 mM NaCl were added to the reaction of MPO cleavage on thio sites in NaAc-HAc buffer (5 mM NaAc-HAc, pH 6.0, 10 mM NaCl). This enzyme cleavage condition was referred to a well-established method in the reported literature.[4] The experimental results show that when the target substance MPO is present, the hairpin structure of KS-M is destroyed, which activates the trans-cleavage activity of CRISPR/Cas12a, giving a higher fluorescence signal. Therefore, the experiment with MPO verified that the CRISPR/Cas12a biosensor was applicable to other enzymes with specific cleavage sites.

2.7 UGI inhibitor analysis

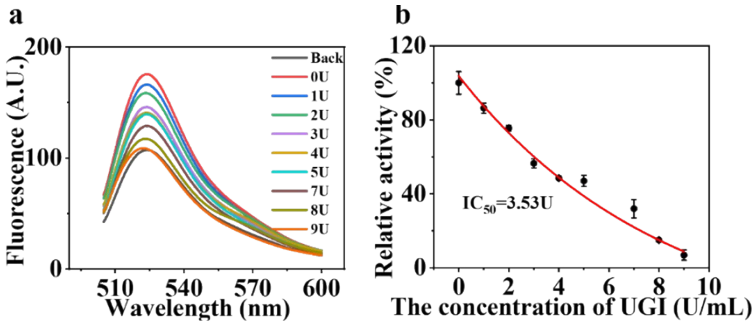

Fig.S9. (a) The fluorescence signal curves of different concentrations of UGI were added. **(b)** Relationship diagram of relative inhibitory activity of UGI on UDG at different concentrations. (The target concentration of UDG was 1 U/mL. Relative activity (%): /F_{UGI}). Error bars represent the standard deviation of three repetitive experiments.

To evaluate the applicability of UDG biosensors in UDG inhibition assays, various concentrations of UGI (0, 1, 2, 3, 4, 5, 7, 8, and 9 U/mL) were selected for experimental validation. The results demonstrate that the fluorescence signals gradually decrease with increasing UGI concentration (Fig. S9a). As shown in Fig. S9b, in the absence of UGI, the relative fluorescence intensity reaches nearly 100%. When the UGI concentration was increased to 9 U/mL, UGI almost completely inhibited UDG activity. Based on this data, the IC_{50} was calculated to be 3.53 U/mL.

2.8 UDG expression in cancer cells

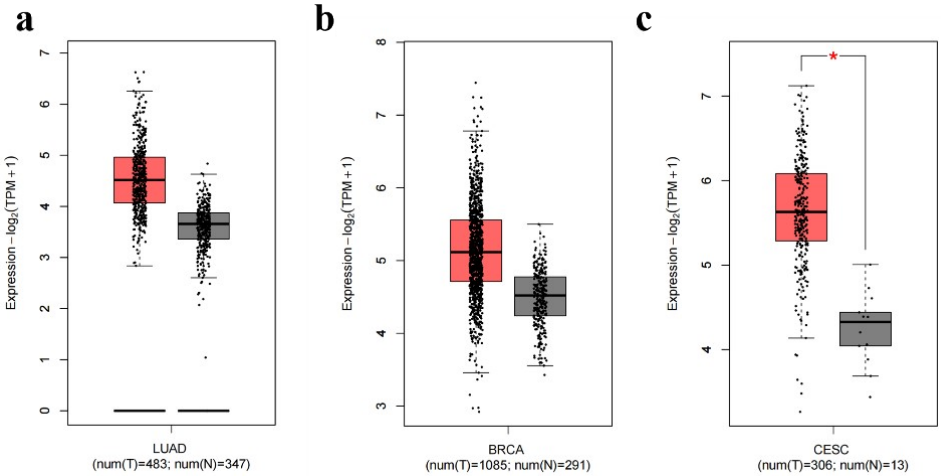

Fig.S10. The overexpression level of UDG in cancer cells checked on the GEPIA2 website. **(a)** Lung Adenocarcinoma (LUAD), **(b)** Breast Cancer Susceptibility Gene (BRCA), **(c).** Cervical Squamous Cell Carcinoma (CESC).

2.9 Detection of UDG activity in cancer cell lysate

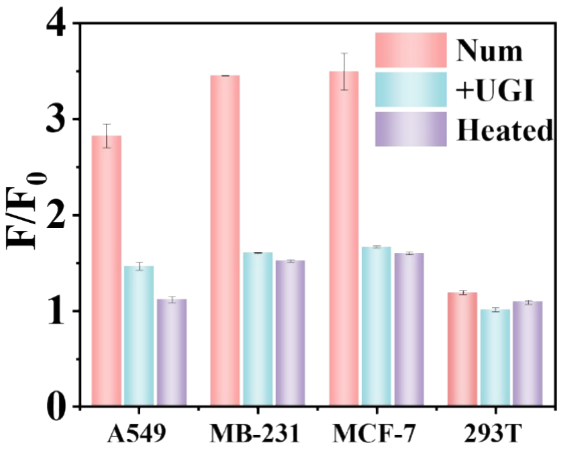

Fig.S11. UDG was directly detected in A549, MB-231, MCF-7, and 293T cell lysates, and the signal-to-noise ratio was detected after the UGI inhibitor was added and inactivated cell lysates were heated. Each group of samples were run in parallel three times (error bars n=3). Error bars represent the standard deviation of three repetitive experiments.

2.10 Cas12/13 nucleic acid strips to validate three target sensors

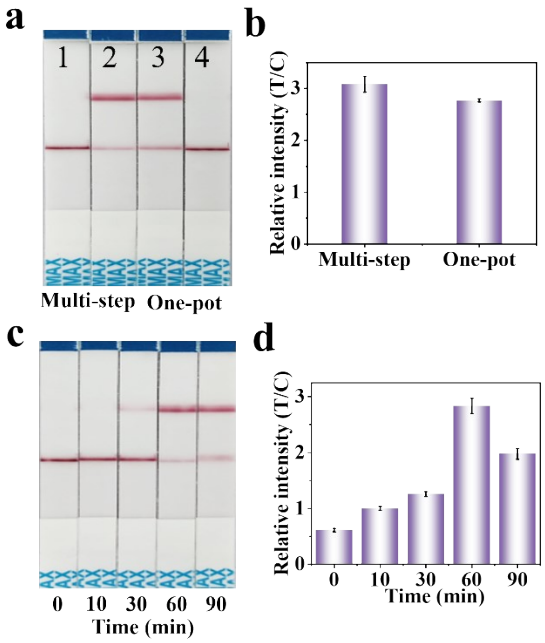

Fig.S12. **(a-b)** The test strip detection results **(a)** and corresponding T/C values **(b)** of multi-step and one-step (test strip 1 and 4 are the results without HPV-16, test strip 2 and 3 are the results with HPV-16). **(c-d)** Results of test strips **(c)** and corresponding T/C values **(d)** at different reaction times (0, 10, 30, 60, 90 min). The target concentration of HPV-16 was 1 μM. Error bars represent the standard deviation of three repetitive experiments.

Table S4. Recovery of HPV-16 detection in serum from human samples

Additon (μmol/L)	Detection (μmol/L)			Recovery (%)	RSD (%)
	1	2	3		
0.4	0.42	0.4	0.38	100.28	5.41
0.8	0.95	0.89	0.89	113.75	3.81
1.2	1.27	1.31	1.23	105.83	3.15

Each group of samples were run in parallel three times (error bars n=3)

Table S5. Detection of recovery of KAN in pure milk and lake water

Add (μmol/L)		Detection (μmol/L)			Recovery (%)	RSD (%)
		1	2	3		
pure milk	5	4.57	4.67	4.5	91.60	1.07
	20	21.49	20.58	20.31	103.97	1.72
	40	38.14	41.24	41.15	100.44	2.53
lake water	5	5.39	5.75	5.57	111.40	3.23
	20	20.86	20.76	20.58	103.67	1.36
	40	39.69	40.61	39.14	99.53	1.86

Each group of samples were run in parallel three times (error bars n=3)

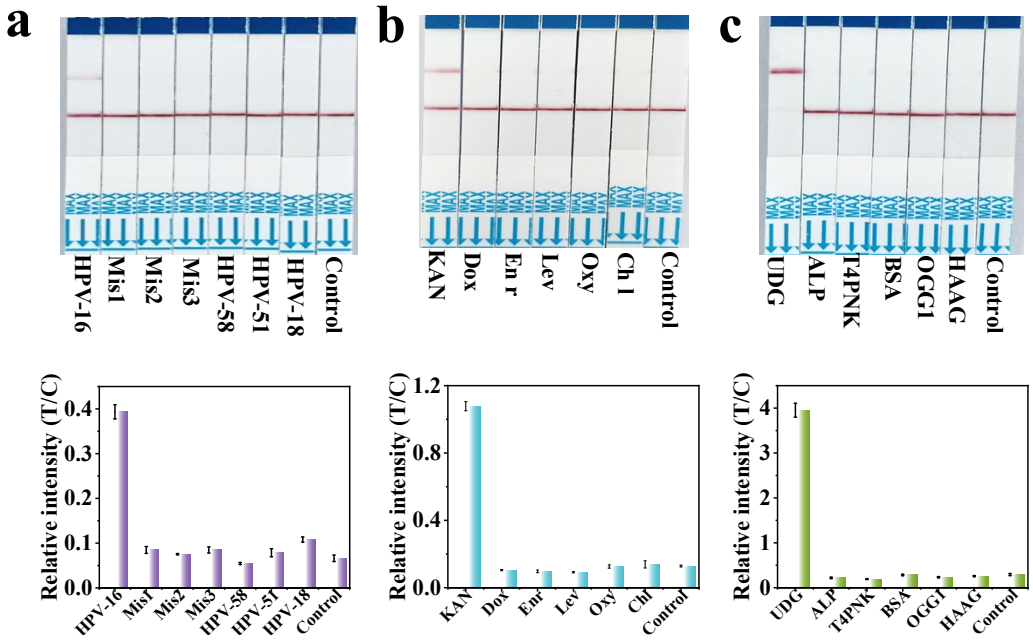

Fig.S13. **(a)** HPV-16-specific test strip detection results (above) and corresponding relative T/C intensity values (below) (C_{target}=2 μM). **(b)** KAN-specific test strip detection results (above) and corresponding relative T/C intensity values (below) (C_{target}=5 μM). **(c)** UDG-specific test strip detection results (above) and corresponding relative T/C intensity values (below) (C_{target}=40 U/mL). Error bars represent the standard deviation of three repetitive experiments.

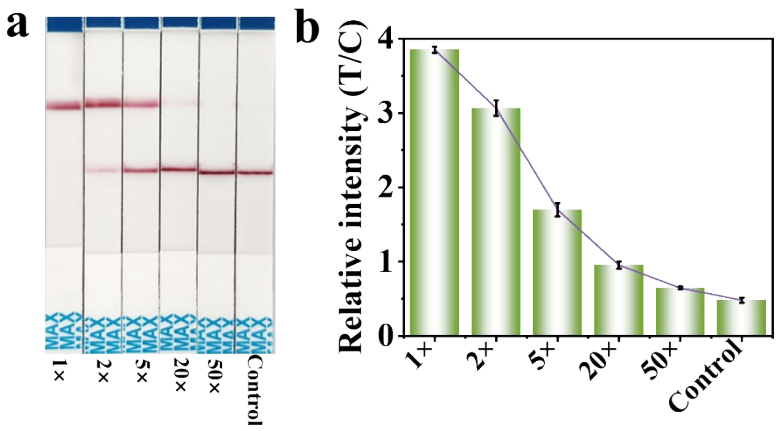

Fig.S14. **(a)** Test strip results and **(b)** corresponding relative T/C intensity values of MCF-7 cell lysis buffer diluted at various concentrations (undiluted, 2×, 5×, 20×, 50×, and blank). Each group of samples were run in parallel three times (error bars n=3). Error bars represent the standard deviation of three repetitive experiments.

Table S6. The LFA proposed in this study was compared with existing point-of-care testing (POCT) methods.

Methods	Amplification	Enzyme	Target	Time	LOD	Reference
CRISPR-distance-based biosensor	SDA	Yes	miRNA	2 h	6.28 pM	[5]
(CRISPR/Cas12a-Responsive Indicators@RCA hydrogels	RCA	Yes	genetic	5 h	2 copies/μL	[6]
CRISPR-CHLFA	RPA	No	SASR-CoV-2	1 h	1–10 copy of target	[7]
CRISPR-LFA/PGM	RAA	Yes	invA gene of Salmonella	2 h	33 CFU/mL, 20 CFU/mL	[8]
CRISPR-PGM	No	Yes	AFP	2.5h	10 ng/mL	[9]
CRISPR-LFA	No	No	Nucleic Acid/Small Molecule/Protein	<2 h	LOD_{HPV-16}=27 nM, LOD_{KAN} = 0.82 μM and LOD_{UDG} = 0.15 U/mL	This work

Table S7. Three methods for detecting the target were compared.

Target	Model	LOD	Range	Reference
HPV-16	electrochemical	18.13 nM	18.75-250 nM	[10]
HPV-16	electrochemical resistive	2.39 nm	5-20 nM	[11]
HPV-16	Keggin-type polyoxometalate (SiW12)-grafted CdS quantum dots -Au NPs	0.8 nM	15-130 nM	[12]
KAN	Nanomaterials-based bioinspired enzyme mimics	15.28 nM	15.28 nM-46.14 nM	[13]
KAN	fluorescence and colorimetric signals	7.3 nM and 14.5 nM	50-1000 nM 100-800 nM	[14]
KAN	fluorescence resonance energy transfer (FRET)	18.9 nM	0.05–50 nM	[15]
UDG	UDG-REtarded CRISPR	9.17×10^{-4} U/mL	0.001 to 1 U/mL	[16]
UDG	electrochemical	0.0079 U/mL	0.01-10 U/mL	[17]
UDG	intramolecular inhibitory effect of the adjacent base-pair (InE(N:N)	0.003 U/mL	0 - 1.0 U/mL	[18]
HPV-16/KAN/UDG	Fluorescence and LFA	Fluorescence : HPV-16:0.0299	Fluorescence: HPV-16: 0.1 -50 nM	This work

		nM，KAN:0.156 nM，UDG:0.0012 U/mL LFA: LOD_{HPV-16}=27 nM LOD_{KAN}= 0.82 μM LOD_{UDG}= 0.15 U/mL	KAN: 10 - 100nM UDG: 0.005 - 1 U/mL LFA: HPV-16:0.1-1.2 μM KAN: 1-40 μM UDG: 0.25-40 U/mL	

1. Q.-N. Li, D.-X. Wang, G.-M. Han, B. Liu, A.-N. Tang and D.-M. Kong, *Analytical Chemistry*, 2023, **95**, 15725-15735.
2. C. McFarlane and J. Murray, *Bio-Protocol*, 2020, **10**.
3. S. J. Klebanoff, A. J. Kettle, H. Rosen, C. C. Winterbourn and W. M. Nauseef, *Journal of Leukocyte Biology*, 2013, **93**, 185-198.
4. J.-Y. Ma, B. Liu, S. Raza, H.-X. Jiang, A.-N. Tang and D.-M. Kong, *Sensors and Actuators B: Chemical*, 2023, **376**.
5. S. Feng, H. Chen, Z. Hu, T. Wu and Z. Liu, *ACS Applied Materials & Interfaces*, 2023, **15**, 28933-28940.
6. R. Zhao, Y. Tang, D. Song, M. Liu and B. Li, *Analytical Chemistry*, 2023, **95**, 18522-18529.
7. M. Cheng, C. Tan, B. Xiang, W. Lin, B. Cheng, X. Peng, Y. Yang and Y. Lin, *Analytica Chimica Acta*, 2023, **1270**.
8. Y. Wang, J. Cao, P. Du, W. Wang, P. Hu, Y. Liu, Y. Ma, X. Wang and A. M. Abd El-Aty, *Microchimica Acta*, 2024, **191**.
9. Z. Jia, Z. Li and C. Liu, *Sensors and Actuators B: Chemical*, 2023, **390**.
10. D. S. Campos-Ferreira, G. A. Nascimento, E. V. M. Souza, M. A. Souto-Maior, M. S. Arruda, D. M. L. Zanforlin, M. H. F. Ekert, D. Bruneska and J. L. Lima-Filho, *Analytica Chimica Acta*, 2013, **804**, 258-263.
11. J. R. Espinosa, M. Galván, A. S. Quiñones, J. L. Ayala, V. Ávila and S. M. Durón, *Molecules*, 2021, **26**.
12. Y. Cheng, C. Sun, Y. Chang, J. Wu, Z. Zhang, Y. Liu, S. Ge, Z. Li, X. Li, L. Sun and D. Zang, *Frontiers in Bioengineering and Biotechnology*, 2023, **11**.
13. W. Wang, Y. Yin and S. Gunasekaran, *Biosensors and Bioelectronics*, 2022, **218**.
14. Y. Tian, Y. Mou, W. Zhang, Z. Sun, Y. Yin, L. Han, D. Chen, Y. Guo, X. Sun, F. Li and Y. Wu, *Biosensors and Bioelectronics*, 2025, **268**.
15. Y. Zhang, R. Liu, M. M. Hassan, H. Li, Q. Ouyang and Q. Chen, *Spectrochimica Acta Part A: Molecular and Biomolecular Spectroscopy*, 2021, **262**.
16. H. Han, S. H. Jang, J. K. Ahn and C. Y. Lee, *Analytica Chimica Acta*, 2024, **1314**.
17. Zhang H, Zhang L, Jiang J and Y. R., *Analytical sciences*, 2013, **29**, 193-198.
18. Z. Su, Q. Wen, S. Li, L. Guo, M. Li, Y. Xiong, W. Li and J. Ren, *Analytica Chimica Acta*, 2022, **1221**.